Electrical properties of photosensitive heterostructures n–FeS$_2$/p–InSe

I.G.Tkachuk[1], I.G.Orletsky[2], Z.D.Kovalyuk[1], P.D.Marianchuk[2]

[1]Chernivtsi Division of I.Frantsevich Institute of Materials Science Problems, 5 I.Vilde St., 58001 Chernivtsi, Ukraine
[2]Y.Fedkovych National University of Chernivtsi, 2 Kotsubinsky Str., 58012 Chernivtsi, Ukraine

Conditions for production of photosensitive anisotypic n–FeS$_2$/p–InSe heterojunctions by the method of low-temperature spray-pyrolysis of thin films of pyrite on crystalline p–InSe substrates are studied. On the basis of analysis of temperature dependences of direct and reverse VACs (Volt-Ampere Characteristics), the dynamics of the change in energy parameters is established and the role of the energy states at the heterojunction boundary in formation of the contact potential difference is determined. A model of the energy diagram of the heterojunction is proposed, which describes well the electrophysical phenomena observed during the experiment. The mechanisms of formation of direct and return currents through the energy barrier of n–FeS$_2$/p–InSe are determined.

Keywords: spray-pyrolysis, volt-ampere haracteristics, heterojunction, heterostructures.

Исследованы условия изготовления фоточувствительных анизотипных гетеропереходов n–FeS$_2$/p–InSe методом низкотемпературного спрей-пиролиза тонких пленок пирита на кристаллические подложки p–InSe. На основании анализа температурных зависимостей прямых и обратных ВАХ изучена динамика изменения энергетических параметров и установлена роль энергетических состояний на границе гетероперехода при формировании контактной разности потенциалов. Предложена модель энергетической диаграммы, которая удовлетворительно коррелирует с экспериментально наблюдаемыми физическими явлениями на гетеропереходе. Определены механизмы токопереноса при прямом и обратном смещении гетероструктуры n–FeS$_2$/p–InSe.

Електричні властивості фоточутливих гетероструктур n–FeS$_2$/p–InSe. *І.Г.Ткачук, І.Г.Орлецький, З.Д.Ковалюк, П.Д.Мар'янчук.*

Досліджено умови виготовлення фоточутливих анізотипних гетеропереходів n–FeS$_2$/p–InSe методом низькотемпературного спрей-піролізу тонких плівок піриту на кристалічні підкладки p–InSe. На основі аналізу температурних залежностей прямих і зворотних ВАХ встановлено динаміку зміни енергетичних параметрів та з'ясовано роль енергетичних станів на межі гетеропереходу при формуванні контактної різниці потенціалів. Запропоновано модель енергетичної діаграми гетеропереходу, яка добре корелює з експериментальними електрофізичними явищами. Визначено механізми формування прямого та зворотного струмів крізь енергетичний бар'єр n–FeS$_2$/p–InSe.

1. Introduction

Indium mono selenide InSe has the band gap width of $E_g = 1.2$ eV, which is in the range of optimal values for photovoltaic transformation of the solar radiation spectrum in terrestrial conditions. The layered structure of InSe crystals with the weak Van der Waals bonds between the layers provides their advantage over other semiconductors in manufacturing the substrates

for heterostructures avoiding operations of ingot cutting, mechanical and chemical processing of the surface. The use of indium selenide as a base material allows the creation of photosensitive structures of various types: on the basis of the 'metal-semiconductor' contact [1], homotransitions [2, 3] and heterojunctions [4−6].

Iron disulfide FeS$_2$ (pyrite) consists of the elements widespread in nature. Photosensitive structures based on FeS$_2$ have been extensively studied lately [7−9]. Using the iron disulfide films with hole conductivity the straightening heterostructures ZnO/p−FeS$_2$ are manufactured [10], on the basis of n−FeS$_2$, the n−FeS$_2$/M Schottky diodes (M = Pt, Au, Nb) [11] and p-i-nZnO/FeS$_2$/CuI diodes are produced [12].

Thin FeS$_2$ films produced by the method of spray-pyrolysis [13] are characterized by high resistance to the aggressive media exposure and have the bandgap width of $E_g \approx 1.25$ eV close to that of InSe. The peculiarity of their optical properties is the low light absorption coefficient in the long-wavelength area through indirect optical transitions. For the radiation energies $h\nu \sim$ 2.2 eV, at which there is a direct absorption, the transmission coefficient of the films is more than 80 %. Such a feature of the optical properties of the thin FeS$_2$ films creates the prospects of their application as a wide-band front layer in heterostructures.

In this research we present the results of the study of electrical properties and spectral photosensitivity of n−FeS$_2$/p−InSe heterojunction produced by the method of low-temperature spray-pyrolysis of pyrite thin films on p−InSe substrates.

2. Experimental

The n−FeS$_2$/p−InSe structures were constructed using the indium selenide crystals of p-type conductivity grown by the Bridgman technique. The hole electrical conductivity was obtained by doping with an dope of cadmium 0.1 % by weight. According to the data of the Hall effect study, the concentration of charge carriers and their mobility perpendicular to the axis of symmetry C in InSe at temperature of 295 K were equal to $p \approx 10^{14}$ cm^{-3} and $\mu_{pH} \approx 50$ cm^2/(B·c) respectively.

FeS$_2$ films ~ 0.5 μm thick were applied on p−InSe substrates by the technique of low temperature spray-pyrolysis of 0.1 M aqueous solutions of FeCl$_3$·6H$_2$O and (NH$_2$)$_2$CS salts with increased content of the
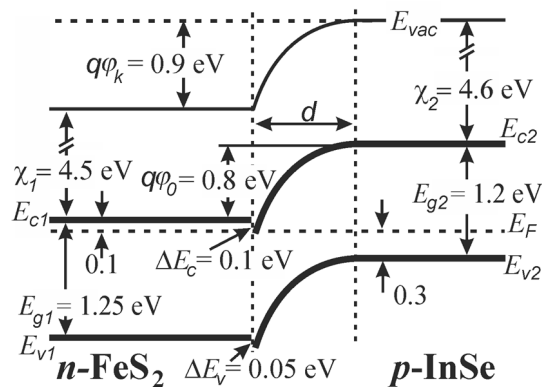
Fig. 1. Energy diagram of n–FeS$_2$/p–InSe heterojunction ($T = 300$ K).

component (NH$_2$)$_2$CS characteristic of sulfide films obtained by this technique [13−17]. To avoid significant thermal action on the p−InSe substrate, the pyrolysis temperature $T_S = 280$°C was chosen, which is in the range of minimum temperatures (~ 250−300°C) for obtaining the high-quality FeS$_2$ films by the technique of spray-pyrolysis [13, 18]. The films of pyrite obtained at this mode possessed a specific electrical conductivity $\sigma = 1.0 \cdot 10^{-2} \Omega^{-1}$ cm^{-1} of n-type at $T = 295$ K. The concentration of charge carriers in the n−FeS$_2$ films is equal to $n = 1.8 \cdot 10^{17}$ cm^{-3}, taking into account the Hall mobility, $\mu H = 0.34$ cm^{2}B^{-1}s^{-1} [19].

Contacts to the base material p−InSe and to the n−FeS$_2$ film were formed using the conductive paste based on silver. Volt-ampere characteristics of the n−FeS$_2$/p−InSe heterostructures were studied on the measuring complex SOLARTRON SI 1286, SI 1255 in the temperature range of $251 < T < 334$ K. Photoconductivity spectra of heterojunctions were measured at room temperature by a mono-chromatometer MDR-3 with resolution of 2.6 nm/mm. For the spectra, normalization was carried out with respect to the flux of photons.

3. Results and discussion

The obtained energy diagram (Fig. 1) was used to analyze the electrical properties of the n−FeS$_2$/p−3InSe heterojunction. It is based on a model with no energy states at the interface and with conservation of the energy parameters of semiconductors (the affinity to electron χ and the band gap width E_g) at the contact boundary (the Anderson model) [20]. For construction of the energy diagram, the values of electron χ affinity (FeS$_2$) = 4.5 eV [21, 22], χ (InSe) = 4.55−4.6 eV [23−26] and

the band gap width E_g (InSe) = 1.2 eV were used [27]. The band gap width of thin films of FeS$_2$ depends on the production conditions. The used value of E_g (FeS$_2$) = 1.25 eV [13] corresponds to the experimental value under the conditions of low-temperature (T_S = 280°C) spray-pyrolysis, at which the n–FeS$_2$/p–InSe heterojunctions were made.

Location of the Fermi level in the restricted zones relative of the bottom of the conduction band for n–FeS$_2$ (δ_1 = 0.1 eV) and the valence band top p–InSe (δ_2 = 0.3 eV) were determined from the expressions for concentration of equilibrium charge carriers of non-degenerate semiconductors [28]:

$$E_C - E_F = \delta_1 = kT \cdot \ln\left(\frac{2}{n} \cdot \left(\frac{2\pi m_n kT}{h^2}\right)^{3/2}\right), \quad (1)$$

$$E_F - E_V = \delta_2 = kT \cdot \ln\left(\frac{2}{p} \cdot \left(\frac{2\pi m_p kT}{h^2}\right)^{3/2}\right), \quad (2)$$

where $m_n = 0.45 \cdot m_0$ [21], $m_p = 0.5 \cdot m_0$ [29] are effective electron masses in FeS$_2$ and holes in InSe, respectively, n and p are concentrations of the main charge carriers in n–FeS$_2$ and p–InSe, E_F — the Fermi level position in the restricted zone.

Distribution of the spatial charge domain (SCD) between semiconductors on the heterojunction was determined by calculating the thickness of the regions in FeS$_2$ and InSe depleted on the main charge carriers using expressions [30]:

$$d_n = \sqrt{\frac{2\varepsilon_0 N_A \varepsilon_n \varepsilon_p \varphi_k}{q N_D(\varepsilon_n N_D + \varepsilon_p N_A)}}, \quad (3)$$

$$d_p = \sqrt{\frac{2\varepsilon_0 N_D \varepsilon_n \varepsilon_p \varphi_k}{q N_A(\varepsilon_n N_D + \varepsilon_p N_A)}}, \quad (4)$$

where q is the electron charge, ε_0 is the dielectric constant (8.85·10^{-12} F·m^{-1}), ε_n = 1.9 [31] and $N_D = n = 1.8 \cdot 10^{17}$ cm^{-3} — the relative dielectric conductivity of donor concentration in FeS$_2$, ε_p = 10.9 [29] and $N_A = p = 10^{14}$ cm^{-3} — dielectric conductivity and acceptor concentration in InSe, $q\varphi_k$ is the height of the potential barrier due to the contact potential difference. The calculated values of d_n and d_p are 1.8·10^{-9} m and 3.27·10^{-6} m, respectively. The ratio of thickness of the depletion regions $d_p \gg d_n$

indicates to concentration of the SCD of n–FeS$_2$/p–InSe heterojunctions in the p–InSe semiconductor.

According to the energy diagram of the n–FeS$_2$/p–InSe heterojunction, the energy barrier $q\varphi_k$ = 0.9 eV in the valence band for p–InSe holes is slightly greater than the energy barrier $q\varphi_0$ = 0.8 eV for electrons in the conduction band n–FeS$_2$ (Fig. 1). Both electrons and holes can take part in the formation of direct and reverse current.

The study of VACs of the n–FeS$_2$/p–InSe heterojunctions at direct and reverse voltages in the temperature range of T = 251–334 K indicated the straightening properties of the structures. The perpendicular direction of the current to the layers plane of the crystal of the p–InSe base area in the n–FeS$_2$/p–InSe heterostructures results in a significant series resistance of R_s. The magnitude of this resistance depends on geometric dimensions of the p–InSe substrate, and at decrease in the area of the heterojunction and significant thickness (~ 2 mm) of the base area it can reach R_s ~ 105 Ω. In the heterostructures studied, the series resistance R_S was determined by cotangent of the inclination angle to the stress axis α (R_S = ctgα = $\Delta V / \Delta I$) of straight sections of the direct branches of the VAC at displacements V > 3 V (R_S = ctgα = $\Delta V / \Delta I$). Correct analysis of processes in the heterojunctions created on the materials with a significant specific resistance is possible if the voltage V_0 applied directly to the SCD of the junction without voltage drop component on the serial resistance $I \cdot R_S$. In this case, the VACs with direct displacement are described by the expression:

$$I(V) = I_s \exp\left(\frac{e(V - IR_S)}{AkT}\right), \quad (5)$$

where V is the total voltage applied to the heterostructure, IR_s is the voltage drop on series resistance of the structure, A is the VAC nonideality coefficient.

The VAC of n–FeS$_2$/p–InSe heterojunctions in the temperature range of T = 251–334 K at direct displacements constructed on the basis of expression (5) are shown in Fig. 2. The exclusion of the series resistance effect enabled to correctly determine the value of the energy barrier φ_0 in the n–FeS$_2$/p–InSe heterojunction by extrapolating the vertical (the condition of $R_s \rightarrow 0$ is satisfied) of the rectilinear regions of the direct VAC. The temperature dependence
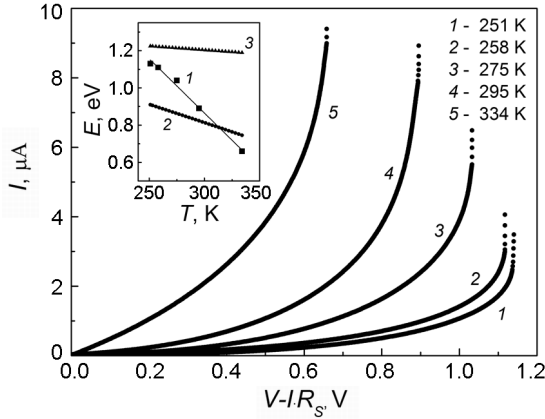
Fig. 2. Direct branches of VAC of n–FeS$_2$/p–InSe heterojunction at different temperatures, taking into account the voltage drop on the series resistance. (Insertion — experimental (*1*) and calculated (*2*) dependence of the height of potential barrier φ_0 in the heterojunction on temperature (*3*) — temperature dependence of the band gap width InSe).

$\varphi_0^{exp} = f(T)$ is shown in Fig. 2 (insertion). The experimentally determined rate of change of the height of a potential barrier with the temperature in the range of $T = 251$–334 K is $d(q\varphi_0^{exp})/dT = -5.82 \cdot 10^{-3}$ eV/K. It comes from the analysis of the energy diagram (Fig. 1) that the height of the potential barrier $q\varphi_k$ due to the contact potentials difference, the dependence on temperature is determined by the ratio.

The value $q\varphi_0$ is determined by the height of the potential barrier for electrons and lesser than the height of the barrier due to the contact potentials difference $q\varphi_k$ by the value of breakdown of conduction zones ΔE_C:

$$q\varphi_0(T) = E_{g2}(T) - kT \cdot \ln\left(\frac{N_C N_V}{n \cdot p}\right). \qquad (6)$$

The rate of change in the height of the barrier for electrons determined by relation (6) taking into account the temperature coefficient of the change in width of the band gap InSe $dE_g/dT \}= -4.2$ eV/K [32] in the temperature interval of $T = 251$–334 K and the dependences on temperature of the main charge carriers concentration and the effective states densities in the permitted zones $N_C(T)$ and $N_V(T)$, is $d(q\varphi_0)/dT = -2.0 \cdot 10^{-3}$ eV/K (Fig. 2, insertion).

The observed difference between the experimental and calculated rate of change with temperature of the potential barrier

height in the n–FeS$_2$/p–InSe heterojunction is within one order and is explained by electrically active states at the interface between the semiconductors [33, 34], which arise as a result of discrepancy of the parameters of the crystal lattices FeS$_2$ and p–InSe. The density of charge states N_{SS} at the interface between the semiconductors is inversely proportional to the square of the distance between dislocations of the discrepancy d ($N_{SS} \approx d^{-2}$), which is determined by the relation:

$$d = \frac{a(\text{FeS}_2) \cdot a(\text{InSe})}{a(\text{FeS}_2) - a(\text{InSe})}, \qquad (7)$$

where $a(\text{InSe})\}= 4.002$ Å [32], and $a(\text{FeS}_2) = 5.42$ Å [35] are the constants of crystalline lattices of InSe and FeS$_2$, respectively. The calculated state density $N_{SS} = 4.3 \cdot 10^{13}$ cm^{-2} is proportional to the N_{SS} values for heterojunctions, in which there is a significant influence of the energy states on the properties [33, 34].

Change in the charge state of the energy states at the interface between the n–FeS$_2$/p–InSe heterojunctions affects the potential barrier height. With increase of temperature, these states are filled by electrons according to the Fermi-Dirac distribution, and a negative charge is localized in the heterojunction. Voltage of the electric field of this charge is oppositely directed to the field strength of the contact potentials difference, which is concentrated in the p–InSe semiconductor. According to the superposition principle, the total electric field in the SCD decreases and, consequently, a smaller experimental value of $\varphi_0^{exp} = 0.66$ V (at $T = 334$ K) is observed compared with the calculated $\varphi_0 = 0.74$ V (see Fig. 2, insertion). When the temperature decreases, the energy states in the heterojunction are released from the electrons; this leads to appearance of a positive charge n in the heterojunction, the electric field of which is in line with the SCD field, and the contact potentials difference increases. With the decrease in temperature up to $T = 251$ K, due to influence of the positively charged states, the greater value of $\varphi_0^{exp} = 1.13$ V is experimentally observed, compared with the calculated one based on the Anderson model $\varphi_0 = 0.91$ V (at $T = 251$ K). We can conclude from the analysis of the temperature dependences of the potential barrier height in the n–FeS$_2$/p–InSe heterojunction (Fig. 2, insertion) that the influence of
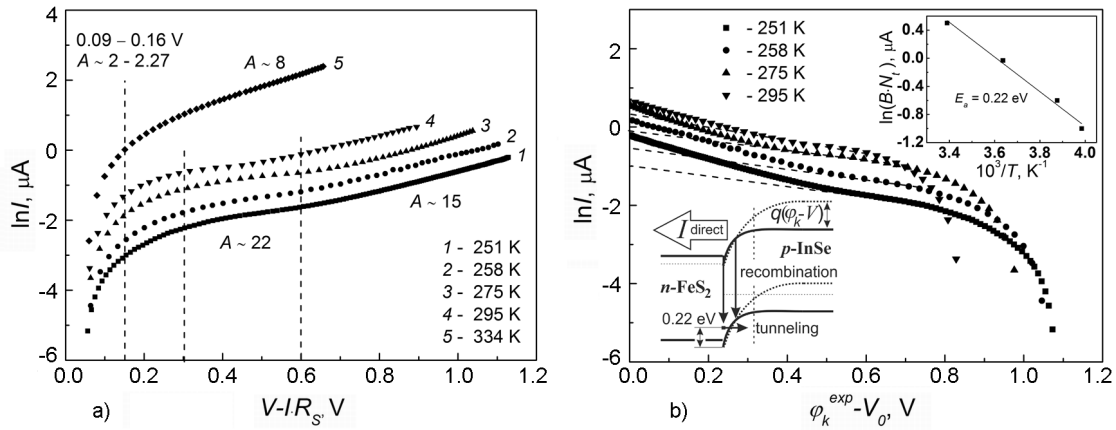
Fig. 3. a) Direct branches of n–FeS$_2$/p–InSe heterojunction VAC in half-logarithmic coordinates at different temperatures T and dependence of series resistance on temperature (insertion). b) Determining the value of $\ln(BN_t)$ and activation energy E_a of traps (insertion) on the boundary of n–FeS$_2$/p–InSe heterojunction.

charge states on the value of φ_0 is not observed only within the temperature interval $T = 310$–320 K. According to these conditions $\varphi_0 = \varphi_0{}^{exp} = 0.78$ V and it is determined by difference between output of the materials and breakdown of the conduction band ΔE_C. At room temperature, the energy barrier is formed by reduced by ΔE_C difference between the outputs and positive charge of the states at the boundary of the heterojunction. The value of φ_0 calculated according to the Anderson model at $T = 295$ K is equal to 0.82 V, (correspondingly, the contact potential difference $\varphi_k = 0.92$ V), while the experimentally observed one is $\varphi_0{}^{exp} = 0.89$ V ($\varphi_k{}^{exp} = 0.99$ V).

To determine the mechanisms of forming direct currents of the heterojunction n–FeS$_2$/p–InSe, the VAC constructed in semilogarithmic scale $\ln I = f(V - IR_s) = f(V_0)$ was used (Fig. 3a). At direct displacements $3kT < qV_0 < 0.16$ V, the slope to the stress axis of dependences $\ln I = f(V_0)$ is characterized by the nonideality coefficient of the VAC $A = 2 - 2.27$. With the decrease of the barrier height at the heterojunction up to value $q\varphi_0 - 0.16$ eV due to the direct displacement, the main mechanism of current formation is recombination of electrons in the SCD located in p–InSe. At direct voltages $0.25 < V_0 < 0.6$, the dependences $\ln I = f(V_0)$ obtained within the temperature interval $T = 251$–295 K are characterized by the coefficient $A \approx 22$. Such great values of A are observed in the p–Ge/n–Si heterojunctions ($A = 24.9$–29.4) [30] with the energy profile of the zone diagram similar to that

of n–FeS$_2$/p–InSe ones, and are the result of formation of direct currents by the transition of electrons to the states in the band gap at the boundary of the heterojunction and their further tunneling in the valence band of the p-type conductivity semiconductor. In the investigated n–FeS$_2$/p–InSe structures, the transition of electrons to the states and their further tunneling in the valence band of p–InSe are most pronounced at the temperatures $T = 251$–295 K and the direct voltages up to 0.6 V. At $V_0 > 0.6$ V, the coefficient $A \approx 15$, that indicates the mixed mechanism of current transfer — i.e. the transition of electrons to the states with further tunneling and recombination of electrons in the SCD. The first component of the current associated with tunneling is limited by the concentration of states at the boundary of the heterojunction and at $V_0 \approx 0.6$ V it turns to saturation. While increasing the direct voltage, the concentration of electrons displaced from n–FeS$_2$ to the heterojunction increases, and some of them form a current due to recombination in the SCD.

For the dependence of $\ln I = f(V_0)$ of the heterojunction n–FeS$_2$/p–InSe at the temperature $T = 334$ K (Fig. 3a) there is no region with clearly expressed tunnel component of the direct current. Within the voltage range $0.25 < V_0 < 0.6$ V, the coefficient $A = 8.3$. At the temperature increase up to $T = 334$ K, the concentration of free states at the boundary of the heterojunction according to the Fermi-Dirac distribution decreases, thus the electronic transitions from the conduction band to these states and the
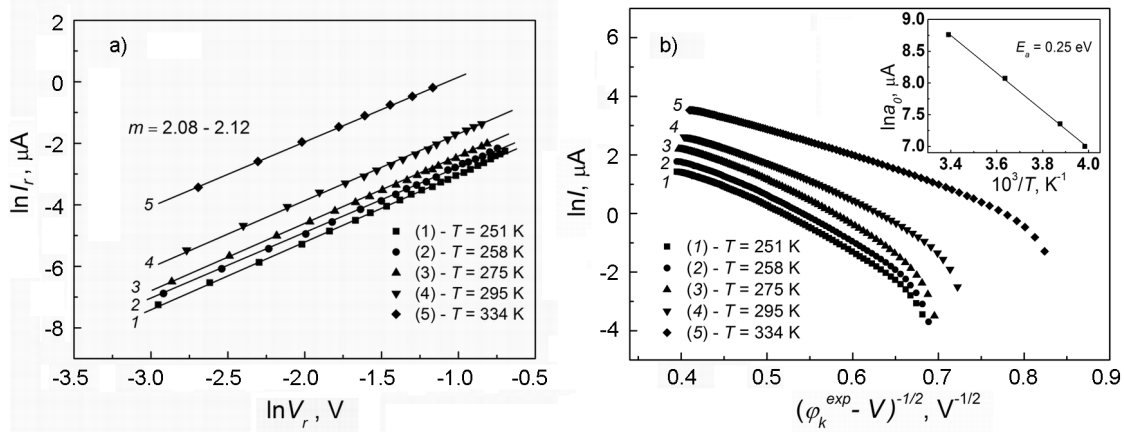
Fig. 4. a) Reverse branches of n–FeS$_2$/p–InSe heterojunctions VAC at voltages $-0.5 < V < 0$ V. b) VAC of n–FeS$_2$/p–InSe heterojunction with inverse displacement $V_r > 0.5$ V at different temperatures T and temperature dependence of a_0 parameter (insertion).

tunneling will also decrease. The recombination component of the direct current at $T = 334$ K increases due to increase in the electrons concentration in n–FeS$_2$. Decrease in the order of the series resistance of the n–FeS$_2$/p–InSe heterostructure with the increase of temperature from 251 to 334 K is characterized by activation energy $E_a = 0.21$ eV, which is identical to the activation energy of the thin FeS$_2$ films [13]. Resistance of the p–InSe substrates, according to the results of TiN/p–InSe structures study [4], does not change in the temperature range under study.

At capture of electrons by traps in the band gap zone at the interface between the heterojunction of n–FeS$_2$/p–InSe and their further tunneling into the valence band p–InSe, the direct current is described by the expression [30]:

$$I(V) = BN_t \exp[-\alpha(\varphi_k - V)], \qquad (8)$$

where B — the constant, N_t — concentration of traps in the band gap zone, α is the value which depends on the effective mass of electrons on the localized states in the band gap zone at the heterojunction boundary, dielectric conductivity and concentration of the acceptor impurity. Since the filling of electronic traps is determined by the Fermi-Dirac distribution function, BN_t exponentially depends on the temperature, while the activation energy corresponding to the traps location relatively to the maximum height of the barrier for holes in the valence band can be found according to tangent of the inclination angle $\ln(BN_t) =$

$f(103/T)$. The dependences $\ln I = f(\varphi_k - V_0)$ for determining $\ln(BN_t)$ and $\ln(BN_t) = f(103/T)$ by (8) are shown in Fig. 4. Extrapolation to ordinate axis was carried out on the VAC linear sections of the temperature range of $T = 251 - 295$ K with the most clearly defined tunnel component of the current, which corresponds to the maximum values of the coefficient A.

According to the determined activation energy $E_a = 0.15$ eV (Fig. 3b, insertion), the traps that are occupied by the electrons of the conduction band at the heterojunction boundary and tunneled into the valence band of p–InSe are located 0.22 eV above the peak of the energy barrier for holes.

The inverse branches of the n–FeS$_2$/p–InSe heterojunction VAC at temperatures $T = 251 - 334$ K in the range of voltages from $-(0.3–0.5) < V < 0$ V are described by the power law $I \sim V^m$ with the value of $m \approx 2$ (Fig. 4a). This dependence $I = f(V)$ is characteristic of the currents that are limited by spatial charge [36].

At the reverse voltages $V_r > (0.3 - 0.5)$ V the n–FeS$_2$/p–InSe heterojunction VAC is described by the expression [20]:

$$I_{rev}^t = a_0 \exp\left(-b_0\left(\varphi_k^{\exp} - V\right)^{-1/2}\right), \qquad (9)$$

where a_0 is the parameter determined by probability of filling of the energy levels, from which the tunneling takes place, with the electrons, b_0 determines the rate of current change from that of voltage.

According to (9), the VAC in the coordinates $\ln I_{rev}^t = f(\varphi_k^{exp} - V)^{-1/2}$ is linear

(Fig. 4b). A slight decrease in inclination angle of the linear regions of the presented dependence at higher temperatures under study is related to the change in the effective density of states in the conduction band n–FeS$_2$ to which the tunneling is carried out, and decrease in the width of the band gap zone of pyrite due to temperature increase. The temperature dependence of a_0 parameter enables to determine (in the first approximation $a_0 \sim -E_a/kT$ [37]) the occurrence depth of the level in the band gap zone of p–InSe, from which the tunneling of electrons occurs. The value of a_0 is obtained by extrapolating the linear regions $\ln I^t_{rev} = f(\varphi_k^{exp} - V)^{-1/2}$ to ordinate axis. The location depth of the level determined from the temperature dependence in the range of 251 $< T <$ 295 K of a_0 parameter (Fig. 4b, insertion), amounts to 0.25 eV relative to the p–InSe valence band top. The obtained value agrees with the occurrence depth of $E_A =$ 0.25 – 0.26 eV of the acceptor levels of the doped Cd p–InSe [38]. The value of a_0 parameter at $T =$ 334 K is lower than that for temperatures of 251 $< T <$ 295 K. This indicates that the levels with lesser probability of filling by electrons participate in the tunneling, that is, the levels that are located deeper in the bandgap than the acceptor ones ($E_T > E_A$). Such deep levels in the indium selenide ($E_T =$ 0.46 – 0.49 eV) are created by the dope of Cd [38].

The spectral dependence of the quantum efficiency at illumination of the n–FeS$_2$/p–InSe heterostructure from the side of FeS$_2$ film covers the photon energy range of 1.2 to 3.1 eV with the maximum at 2.8 eV (Fig. 5). The long-wave edge of photosensitivity corresponds to the energy of quanta of 1.2 eV and is determined by the edge of fundamental absorption in p–InSe. The n–FeS$_2$ film applied on p–InSe is a nondirect gap semiconductor [13] and light absorption in it at the energies slightly higher than the band gap ($E_g =$ 1.25 eV) is characterized by a small absorption coefficient $\alpha \sim$ 10^3 cm^{-1}. At the quanta energy $h\nu =$ 1.5 eV, the absorption coefficient of FeS$_2$ $\alpha \sim$ 10^{-4} cm^{-1} and $\sim$ 60 % of radiation penetrates to the n–FeS$_2$/p–InSe heterojunction boundary through the film with thickness $d =$ 0.5 μm. The direct optical junctions with high $\alpha \sim$ 10^5 cm^{-1} in FeS$_2$ begin at absorption of quanta $h\nu \sim$ 2.2 eV. At the radiation energy $\sim$ 2.8 eV, which corresponds to the maximum of photoconductivity of the n–FeS$_2$/p–InSe heterostructure,
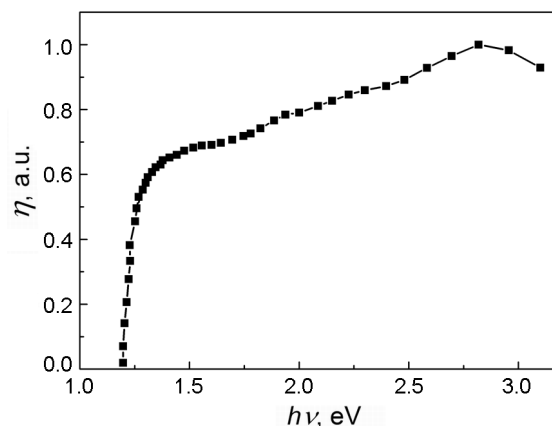
Fig. 5. Spectral dependence of relative quantum efficiency of n–FeS$_2$/p–InSe heterojunction.

the photogeneration of nonequilibrium charge carriers is completely concentrated in the FeS$_2$ film. At irradiation by quantum energies $h\nu >$ 2.8 eV, the region of the most intense generation of electron-hole pairs approaches to the frontal surface of FeS$_2$, for which a high recombination rate is typical, and photosensitivity of the n–FeS$_2$/p–InSe structures decreases. The total width of the spectrum of the relative quantum efficiency at the half-height $\delta_{1/2}$ is not less than 1.8.

4. Conclusions

Photosensitive n–FeS$_2$/p–InSe heterostructures were obtained by the technique of low-temperature spray pyrolysis of FeS$_2$ films on the surface of p–InSe. The straightening properties of the structures are determined by the energy barrier $q\varphi_0 =$ 0.89 eV (at $T =$ 295 K) for electrons in the conduction band in the heterojunction, which differs from the contact potentials difference $\varphi_k =$ 0.99 V due to distinction of the electron affinities of the contacting materials. The n–FeS$_2$/p–InSe heterojunction SCD is formed due to difference in the output works of the electron from the materials and partial influence of the charged states at the boundary of division. When direct voltages reach up to 0.16, the current flows through the heterojunction due to recombination in the SCD, which is located in near-contact region from the side of p–InSe. At direct displacements of $V >$ 0.16 the basic mechanism of current flow is to capture the electrons trapped at the heterojunction border (energy states by 0.22 eV higher than the valence band peak) with further tunneling in the valence band of p–InSe. The reverse current at the voltages

up to (0.3–0.5) V is limited by the area of spatial charge of free charge carriers. Increase in the reverse voltage above 0.5 V leads to the tunneling of electrons from the energy levels of the *p*–InSe band gap. The wide spectrum of quantum efficiency of *n*–FeS$_2$/*p*–InSe heterostructures 1.2–3.1 eV contributes to the prospect of their use as photoconductors of radiation energy, under the condition that the series resistance is reduced.

References

1. S.I.Drapak, V.B.Orletskii, Z.D.Kovalyuk, *Techn. Phys. Let.*, **29**, 480 (2003).

2. V.A.Khandozhko, Z.R.Kudrynskyi, Z.Kovalyuk, *Semiconduct.*, **48**, 545 (2014).

3. V.N.Katerinchuk, M.Z.Kovalyuk, *Phys. Stat. Sol.(a)*, **25**, 133 (1992).

4. I.G.Orletsky, M.I.Ilashchuk, V.V.Brus, *Semiconduct.*, **50**, 334 (2016).

5. Z.R.Kudrynskyi, Z.D.Kovalyuk, V.N.Katerynchuk, *Act. Phys. Pol. A*, **124**, 720 (2013).

6. V.N.Katerynchuk, Z.R.Kudrynskyi, V.V.Khomyak, *Semiconduct.*, **47**, 943 (2013).

7. S.Middya, A.Layek, A.Dey, P.P.Ray, *J. Mater. Sci. Technol.*, **30**, 770 (2014).

8. L.Luo, W.Luan, B.Yuan, *Energy Proc.*, **75**, 2181 (2015).

9. S.Shukla, N.H.Loc, P.P.Boix, T.M.Koh, *ACS Nano*, **8**, 10597 (2014).

10. S.Kawai, R.Yamazaki, S.Sobue, *APL Materials*, **2**, 032110 (2014).

11. K.Buker, N.Alonso-Vante, H,Tributsch, *J. Appl. Phys.*, **72**, 5721 (1992).

12. Z.Yang, M.Wang, S.Shukla, *Scient. Rep.*, **5**, (2015).

13. I.G.Orletskii, P.D.Mar'yanchuk, E.V.Maistruk, *Phys. Sol. Stat.*, **58**, 37 (2016).

14. I.G.Orletskii, P.D.Maryanchuk, E.V.Maistruk, *Inorg. Mater.*, **52**, 851 (2016).

15. V.V.Brus, I.S.Babichuk, I.G.Orletskyi, *Appl. Opt.*, **55**, 158 (2016).

16. I.G.Orletskii, P.D.Mar'yanchuk, M.N.Solovan, *Phys. Sol. Stat.*, **58**, 1058 (2016).

17. I.G.Orletskii, P.D.Mar'yanchuk, M.N.Solovan, *Tech. Phys. Lett.*, **42**, 291 (2016).

18. C.T.Kao, J.B.Shi, H.W.Lee, F.C.Cheng, *J. Therm. Spray Techn.*, **25**, 580 (2016).

19. M.Morsli, A.Bonnet, L.Cattin, *J. Phys. I France*, **5**, 699 (1995).

20. B.L.Sharma, R.K.Purohit, *Semicond. Heteroj.*, **14**, 451 (1974).

21. A.Ennaoui, H.Tributsch, *Sol. Energy Mater.*, **27**, 461 (1986).

22. G.W.Mudd, S.A.Svatek, L.Hague, *Adv. Mater.*, **27**, 3760 (2015).

23. F.Yan, L.Zhao, A.Patane, P.Hu, *Nanotechnology*, **28**, 25 (2017).

24. M.K,L,Man, A.Margiolakis, S.Deckoff-Jones, *Nat. Nanotech.*, **12**, 36 (2016).

25. S.E.Al Garni, O.A.Omareye, A.F.Qasrawi, *Optik — International Journal for Light and Electron Optics*, **144**, 340 (2017).

26. Z.D.Kovalyuk, O.N.Sydor, V.Katerinchuk, *Semiconduct.*, **41**, 1056 (2007).

27. S.M.Sze, K.Kwok, *Phys. Semiconduct. Dev.*, **13**, 19 (2007).

28. N.Kuroda, Y,Nishina, *Sol. Stat. Commun.*, **34**, 481 (1980).

29. A.G.Milnes, D.Feucht, New York and London: Academic Press), 27 , 36 (1972).

30. D.E.Husk, M.S.Seehra, *Sol. Stat. Commun.*, **45**, 1147 (1978).

31. O.Madelung, *Semiconduct.*, **48**, 23 (2007).

32. V.V.Brus, M.I.Ilashchuk, Z.D.Kovalyuk, *Semiconduct.*, **85**, 1077 (2011).

33. V.V.Brus, I.G.Orletsky, M.I.Ilashchuk, *Semiconduct.*, **2**, 1046 (2014).

34. Y.Xu, M.Schoonen, *Americ. Miner.*, **5**, 543 (2011).

35. A.Lampert Murray, P.Mark, *Current Injection in Solids*, **44**, 24 (1970).

36. P.M.Gorley, Z.M.Grushka, V.P.Makhniy, *Phys. Stat. Sol.(c)*, **44**, 3622 (2008).

37. A.Segura, M.C.Martinez-Tomas, B.Mari, *Apl. Phys. A*, **34**, 249 (2007).